

Microscopia SHG e THG na detecção do câncer



X WORKSHOP TEÓRICO-PRÁTICO DO
INFABIC
17-21 e 24-27 de outubro de 2022

Javier Adur

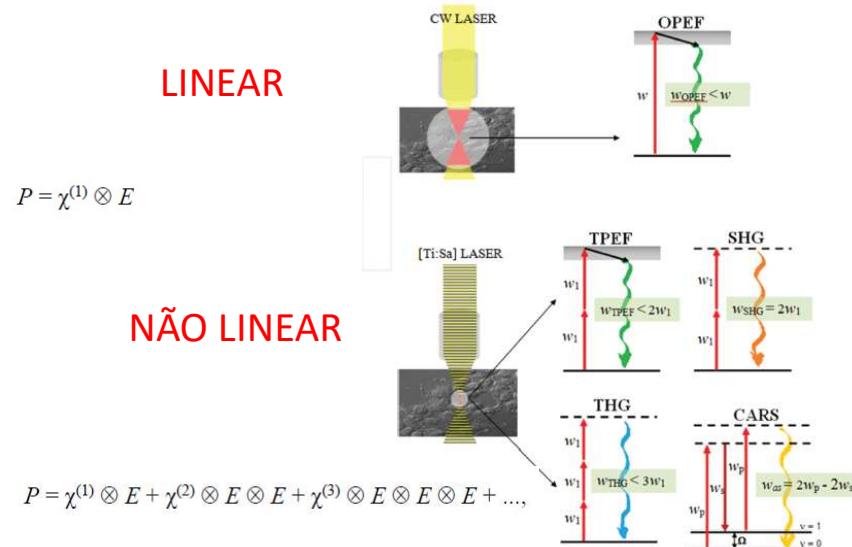
 Facultad de
UNER Ingeniería

CONICET 
Universidad Nacional
de Entre Ríos
I B B

ORGANIZAÇÃO

- ✓ Microscopias não lineares
- ✓ Propriedades das microscopias não lineares
- ✓ Contraste nas microscopia SHG e THG
- ✓ Implementação
- ✓ Aplicações na detecção do câncer

MICROSCOPIAS NÃO LINEARES

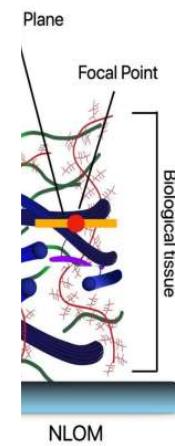


J. Adur et al. (2016) Chapter 6, Nonlinear microscopy techniques.... Intech Open Science

3

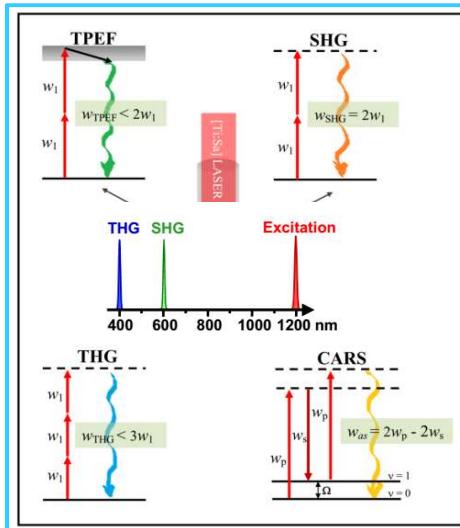
MICROSCOPIAS NÃO LINEARES

As sinais não lineares dependem da probabilidade de encontrar mais de um fóton no espaço e no tempo, o que aumenta dramaticamente no foco de um laser pulsado.

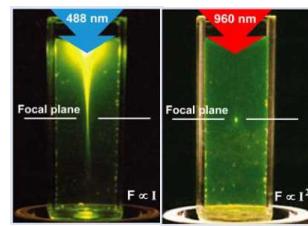


4

PROPRIEDADES



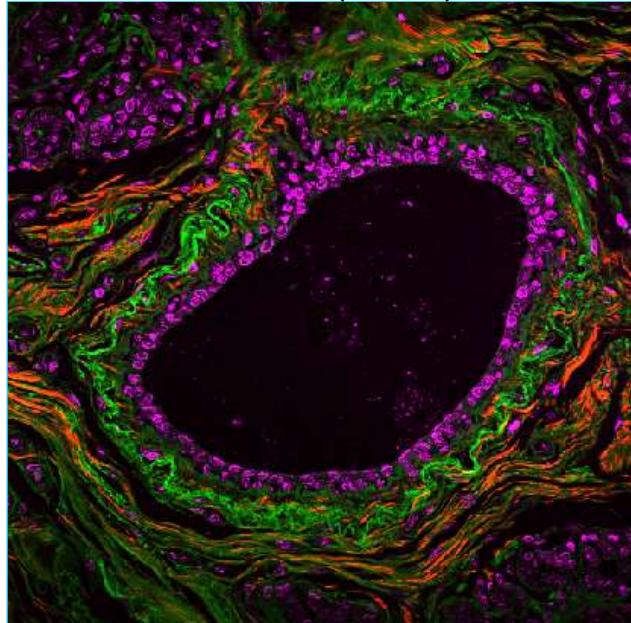
- São processos intrinsecamente confocais
- São processos elásticos e coerentes
- Não precisa de marcadores
- Maior penetração
- Fácil de separar com filtros



J. Adur et al. (2014) Chapter 3, Nonlinear Optics: Fundamentals, Applications.... Nova Science Publishers

5

TPEF+SHG+THG (Mama)



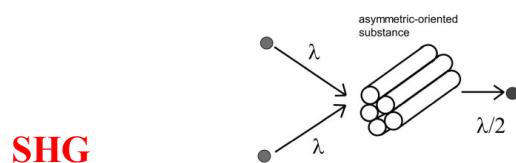
J. Adur et al. (2012) Journal of Biomedical Optics 17(8), 081407

6



MECANISMOS DE CONTRASTE

La microscopía de segundo y tercer armónico se basan en los efectos ópticos que son inducidos por las propiedades físicas inherentes de la muestra.



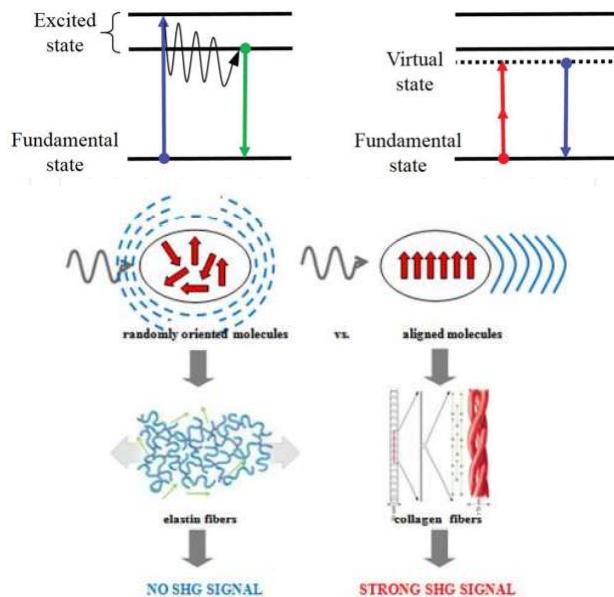
SHG

- Permitido solo en moléculas sin simetría de inversión
- Favorecido en estructuras con alto grado de orientación y organización.

THG

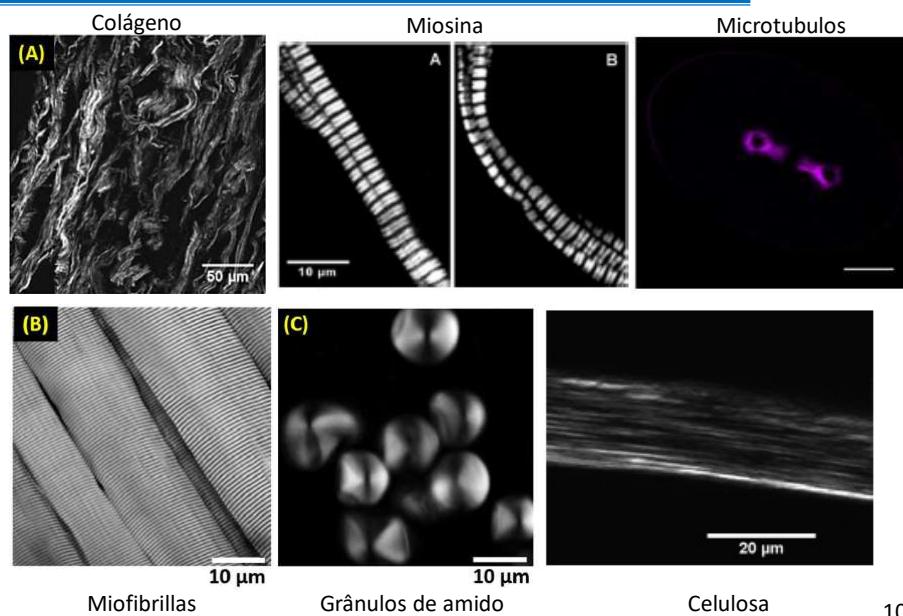
- Permitido en cualquier medio
- Proviene de las interfaces ópticas y las heterogeneidades.

SEGUNDO HARMÔNICO

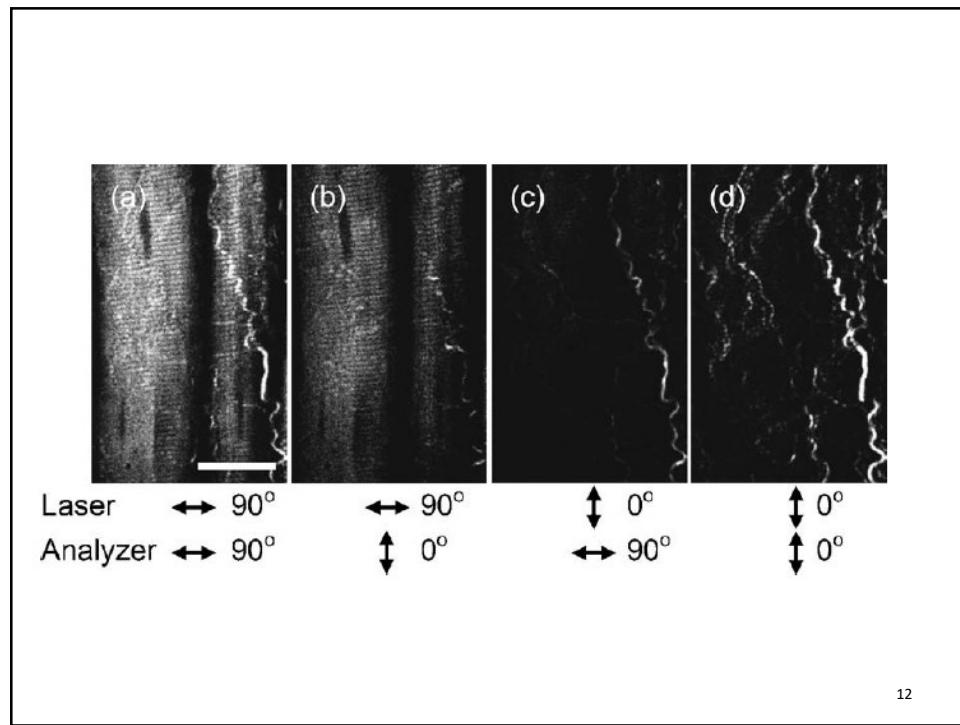
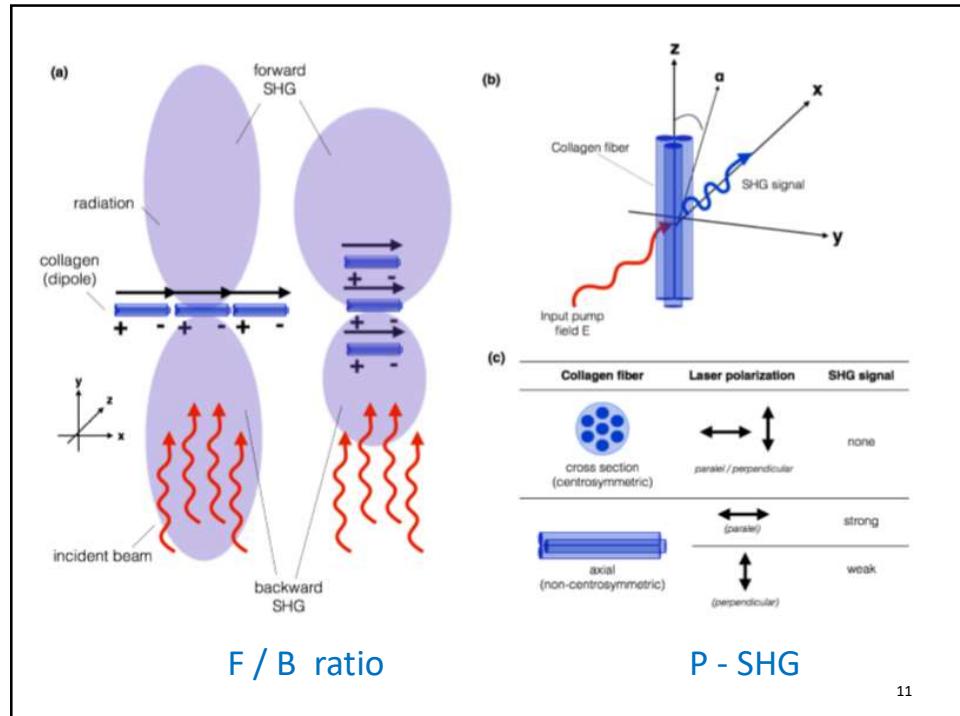


9

SEGUNDO HARMÔNICO



10



CONTRASTE THG

- Permitido em qualquer médio
- Derivado de interfaces e heterogeneidades óticas

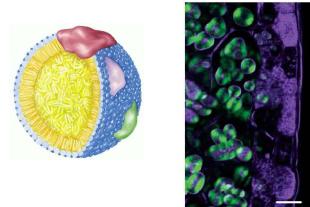
TABLE 4 Optical properties of lipids and glycerol at 1180 nm and comparison with water

	$\alpha = \chi^{(3)} / n_{3\omega} (n_{3\omega} \cdot n_{\omega})$ ($10^{-22} \text{ m}^2 \text{ V}^{-2}$)	$\chi^{(3)}$ ($10^{-22} \text{ m}^2 \text{ V}^{-2}$)	$ \alpha - \alpha_{\text{water}} ^2$	$ \chi^{(3)} - \chi^{(3)}_{\text{water}} ^2$
Water	61.8 ± 3.6	1.68 ± 0.08	0	0
NaCl 1mol/L	63.9 ± 4.2	1.79 ± 0.09	0.012	4.41
Triglycerides	83.7 ± 5.0	2.58 ± 0.5	0.8	480
Triglycerides + cholesterol 1%	83.7 ± 5.0	2.58 ± 0.5	0.8	480
Vegetable oil	90.0 ± 5.0	2.71 ± 0.5	1.1	795
Glycerol	85.2 ± 5.0	2.63 ± 0.5	0.9	550

D. Débarre et al 2006. Nature Methods 30(1): 47-53

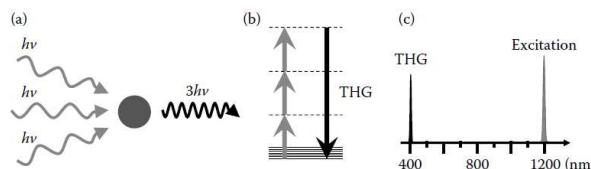
$$I_{\text{THG}} = \left(\frac{3\omega}{2n_{\omega}c} \right)^2 \chi^{(3)} I_{\omega}^3 \int_{z1}^{z2} \frac{e^{i\Delta kz}}{(1 + 2iz/b)^2} dz,$$

O contraste de uma determinada estrutura depende do tamanho da mesma relativo ao volume focal.

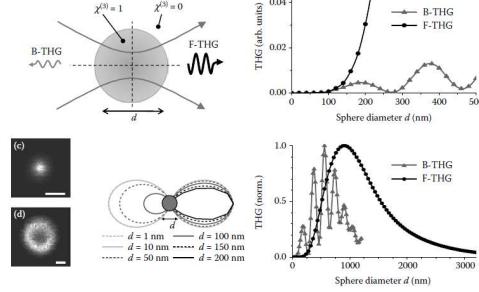


13

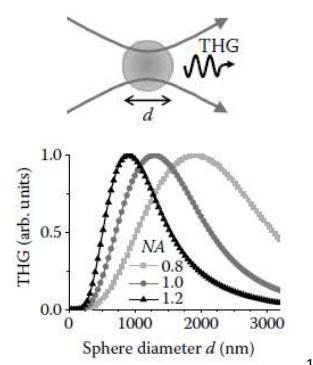
Processo THG



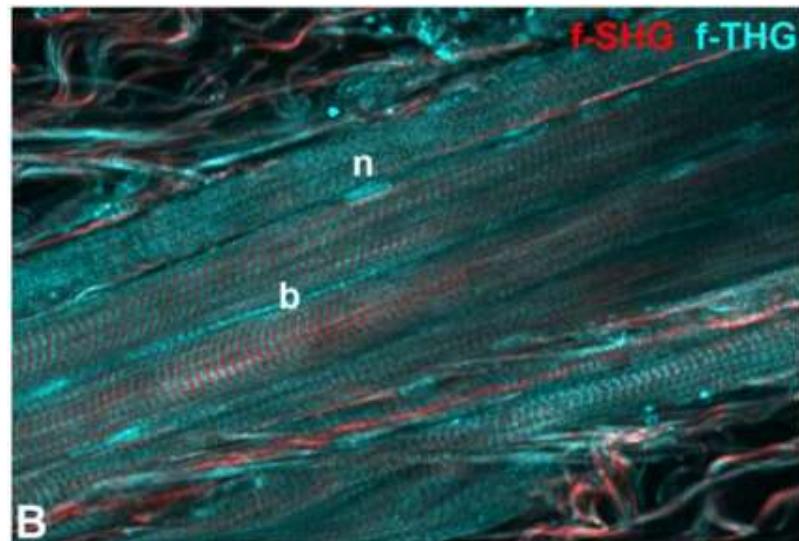
Efeitos de tamanho



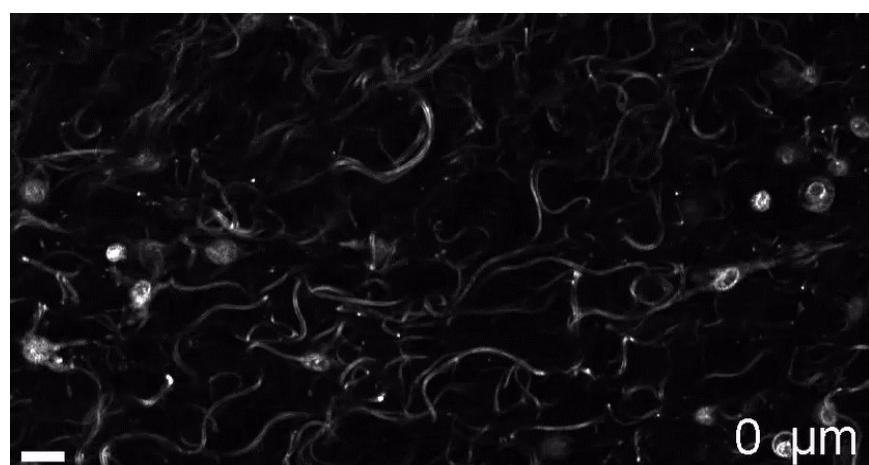
Influência da Excitação NA



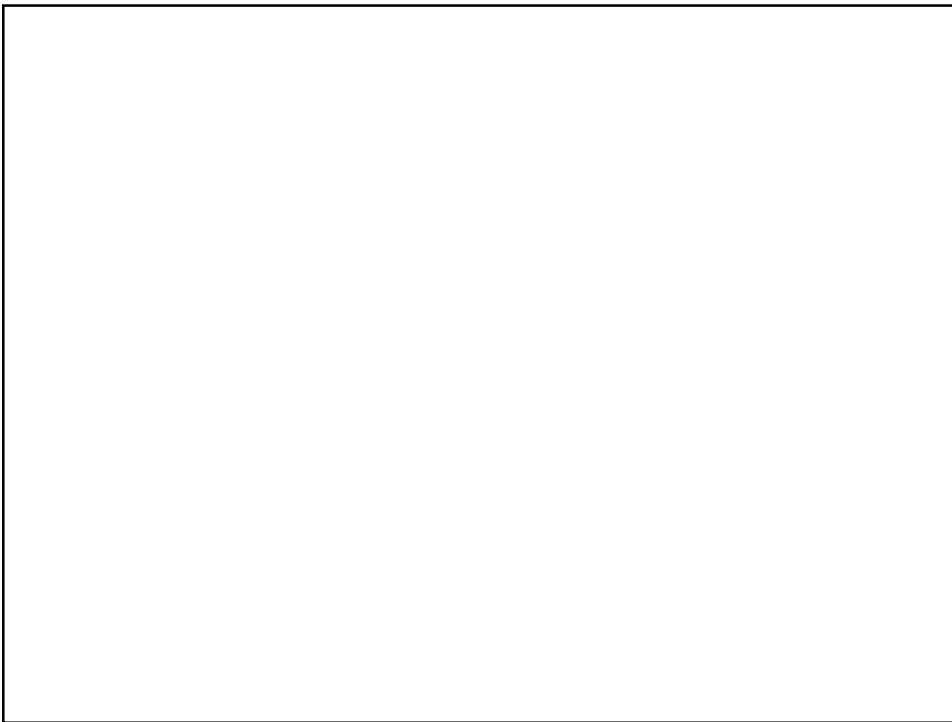
14



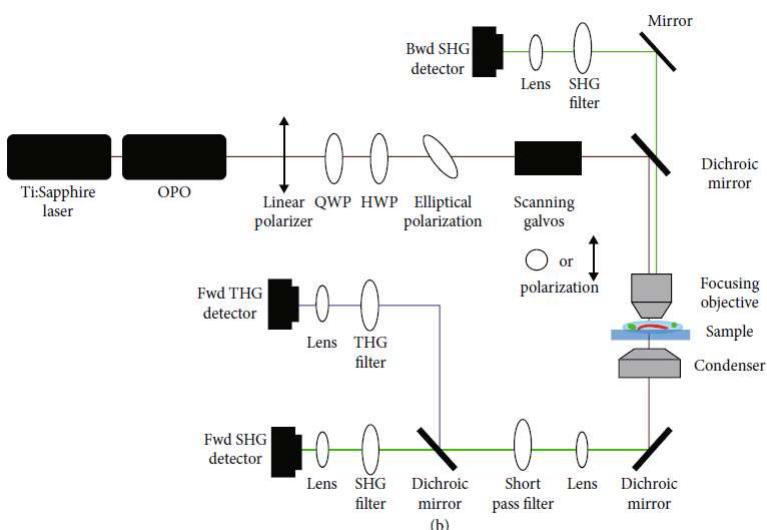
15



16

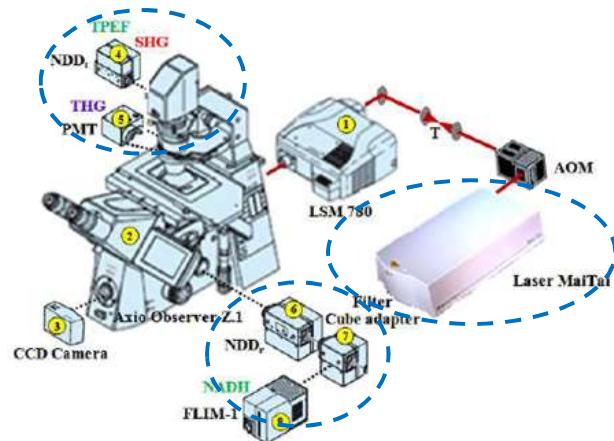


IMPLEMENTAÇÃO



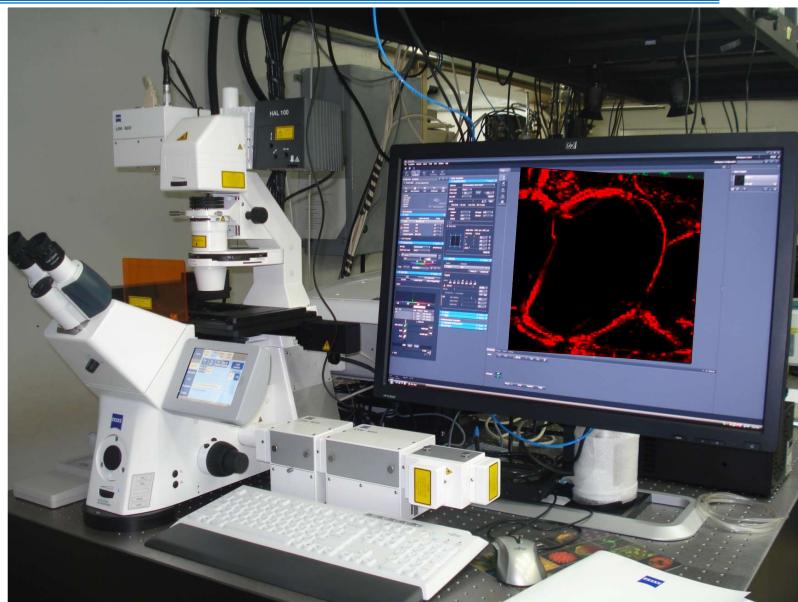
18

IMPLEMENTAÇÃO



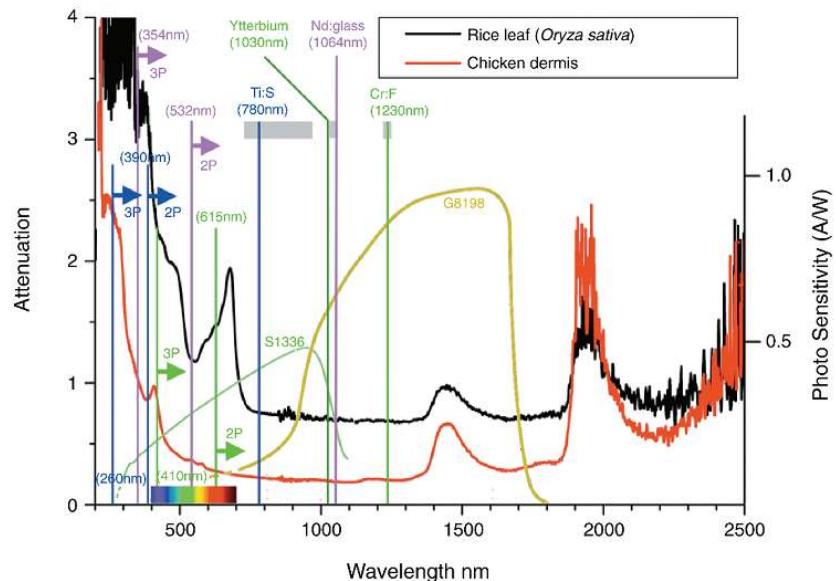
19

IMPLEMENTAÇÃO



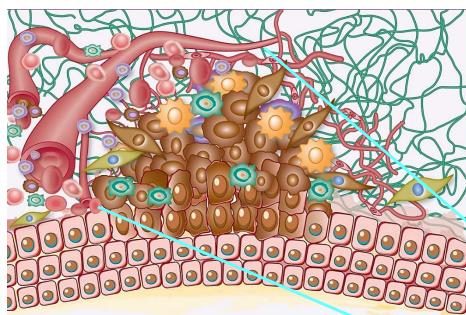
20

IMPLEMENTAÇÃO

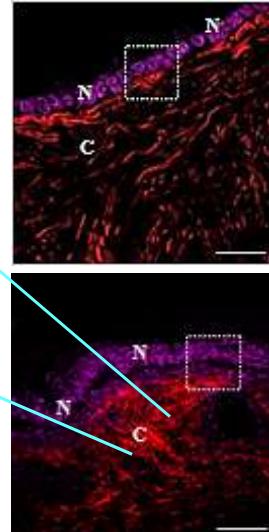


21

APLICACOES NA DETECAO DO CÂNCER



Ioana Berindan-Neagoe and George A. Calin, Clin Canc. Res. 2014



Adur 2014

23

OPEN ACCESS Freely available online

PLOS ONE

Optical Biomarkers of Serous and Mucinous Human Ovarian Tumor Assessed with Nonlinear Optics Microscopies

Javier Adur^{1,2*}, Vitor B. Pelegati¹, Andre A. de Thomaz¹, Mariana O. Baratti⁶, Diogo B. Almeida¹, L. A. L. A. Andrade³, Fátima Bottcher-Luiz⁴, Hernandes F. Carvalho^{5,6}, Carlos L. Cesar^{1,6}

1 Biophotonic Group, Optics and Photonics Research Center, University of São Paulo, São Paulo, Brazil, 2 Microscopy and Spectroscopy Applied to Medicine, Department of Pathological Anatomy, Faculty of Medical and Gynecology, Faculty of Medical Sciences, State University of Cuiabá, Brazil, 3 Department of Pathological Anatomy, Faculty of Medical and Biophysics, Institute of Biology, State University of Cuiabá, Brazil, 4 Photonics Applied to Cell Biology, Caminas, São Paulo, Brazil

J. Biophotonics 1–13 (2012) / DOI 10.1002/jbio.201200108

FULL ARTICLE

Second harmonic generation microscopy as a powerful diagnostic imaging modality for human ovarian cancer

Javier Adur^{1,2*}, Vitor B. Pelegati¹, Andre A. de Thomaz¹, Mariana O. Baratti³, Liliana A. L. A. Andrade⁴, Hernandes F. Carvalho^{3,5}, Fátima Bottcher-Luiz^{3,6}, and Carlos Lenz Cesar^{1,3}

Epithelial Ovarian Cancer Diagnosis of Second-Harmonic Generation Images: A Semiautomatic Collagen Fibers Quantification Protocol

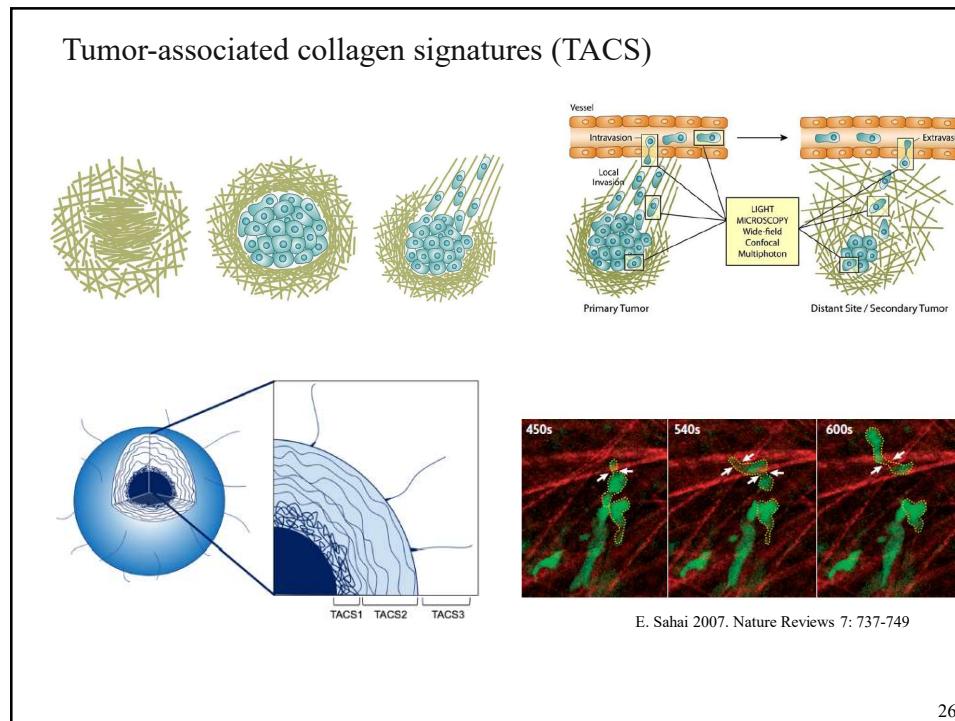
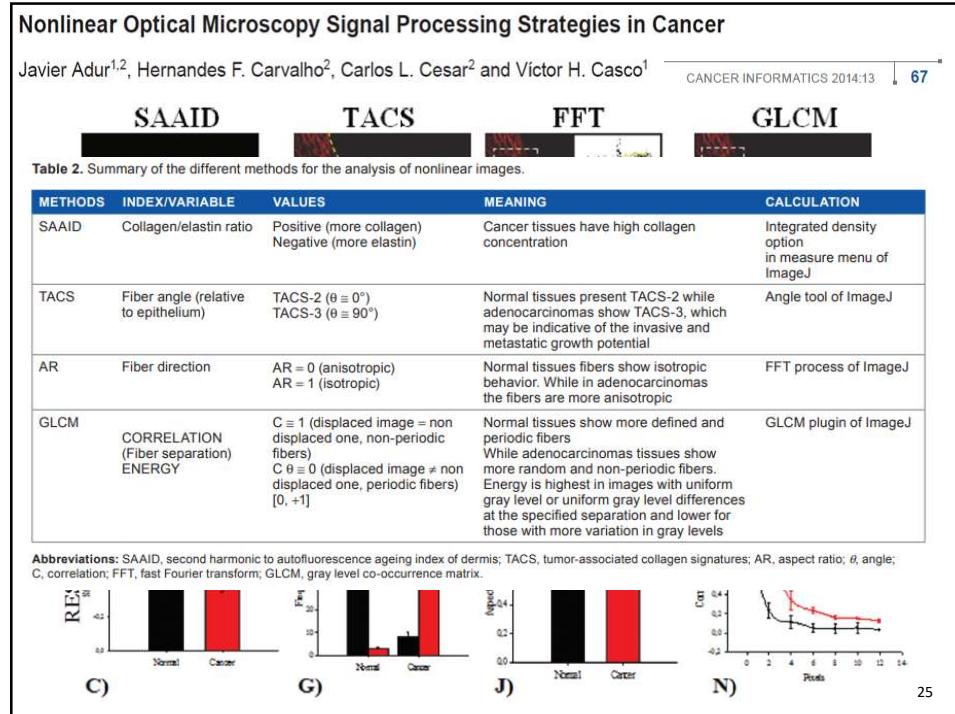
Angel A Zeitouni^{1,2}, Johana SJ Luna³, Kynthia Sanchez Salas³, Luciana Erbes^{1,2}, Carlos L Cesar^{4,5}, Liliana ALA Andrade⁶, Hernandes F Carvahlo^{4,7}, Fátima Bottcher-Luiz^{4,8}, Victor H Casco² and Javier Adur^{1,2,3}

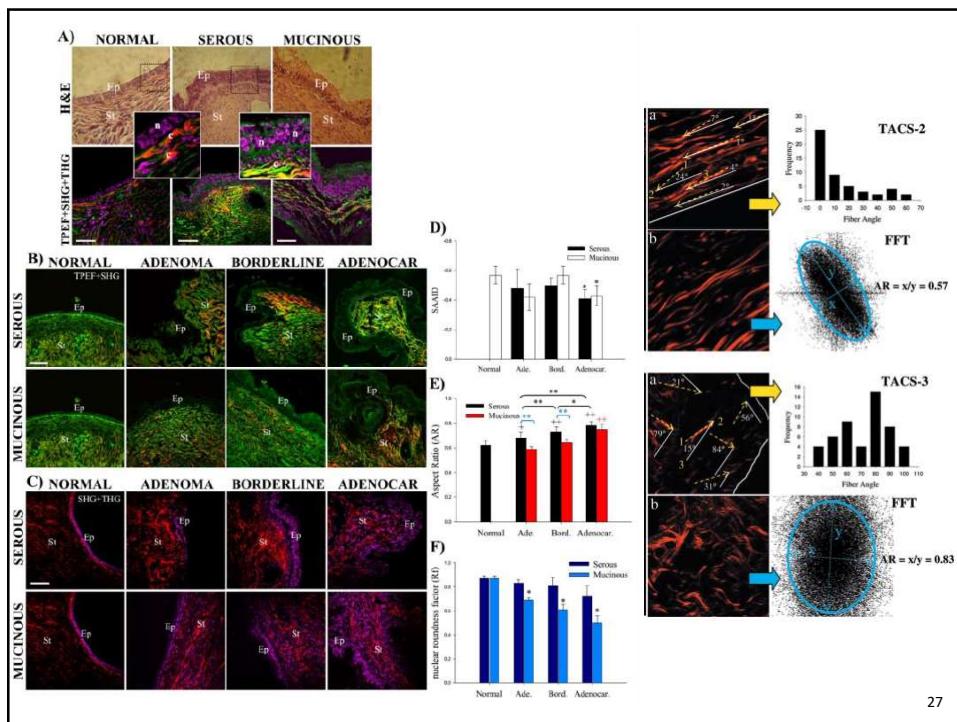
Cancer Informatics
1–12
© The Author(s) 2017
Reprints and permissions:
sagepub.co.uk/journalsPermissions.nav
DOI: 10.1177/1176935117690162
http://jbi.sagepub.com

Journal of BIOPHOTONICS

SAGE

24

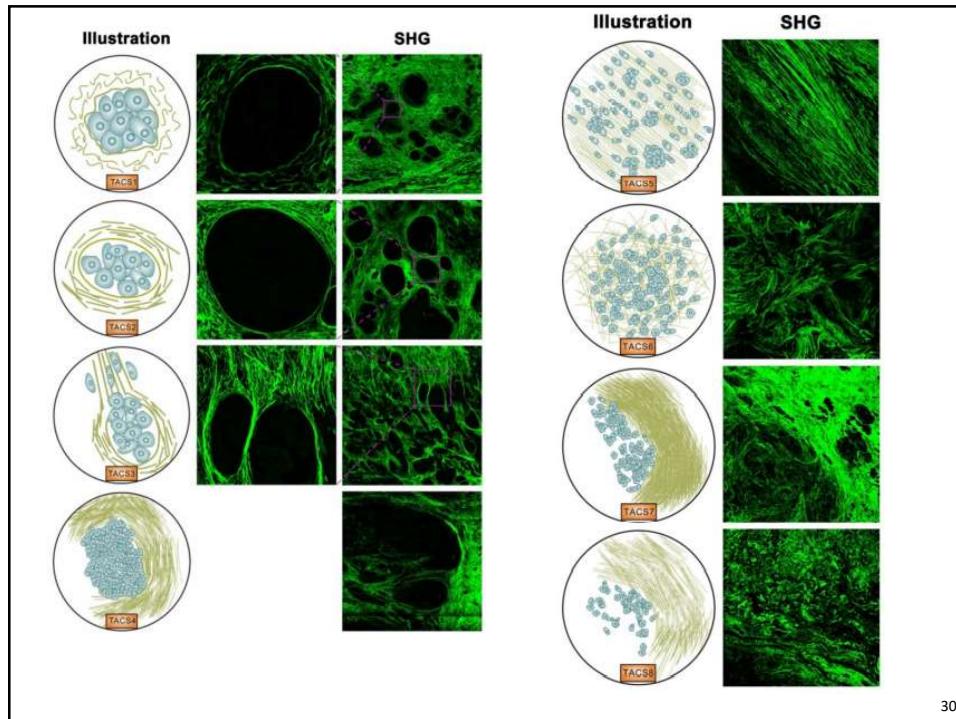
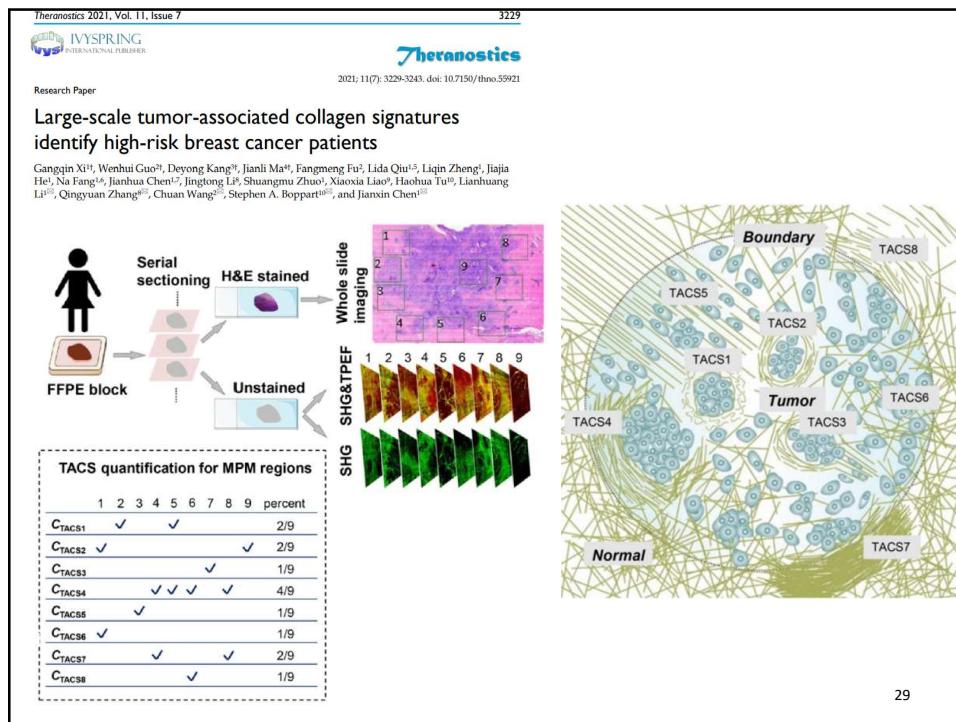


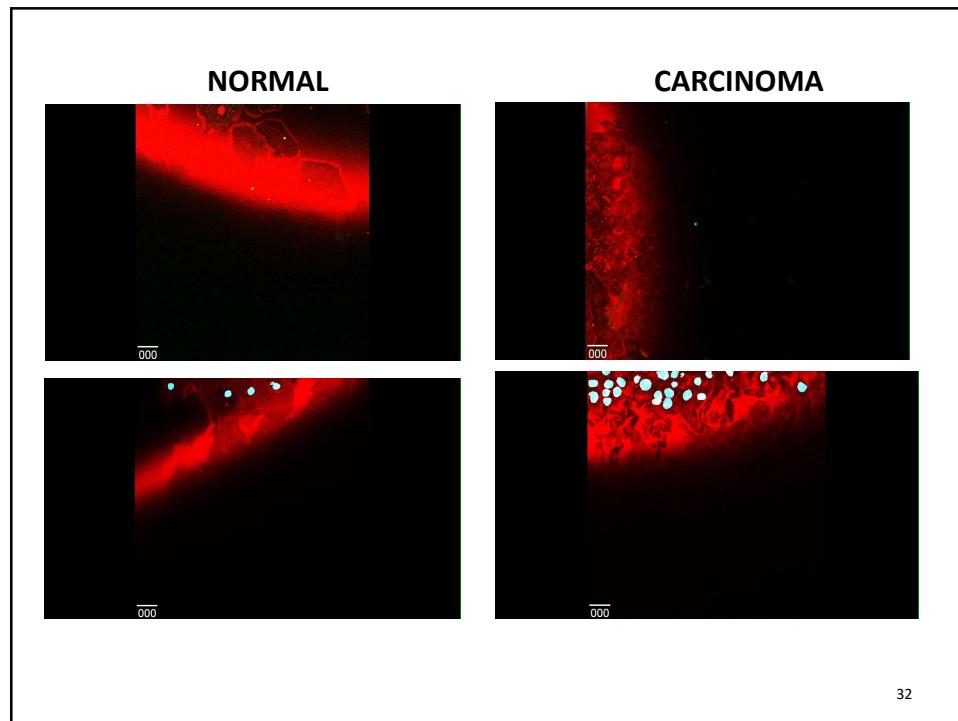
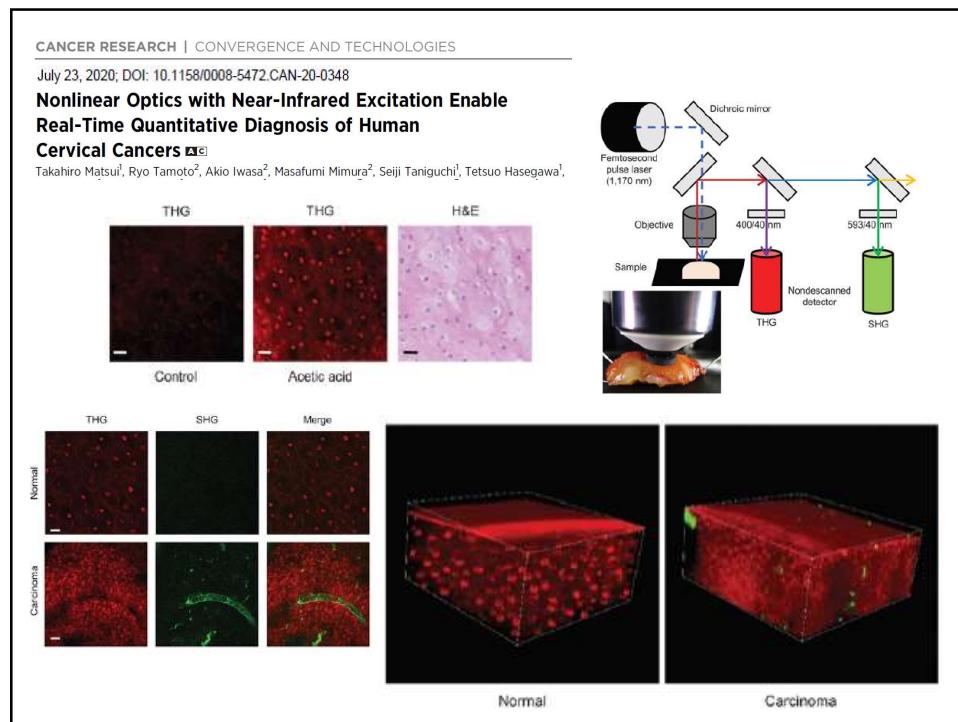


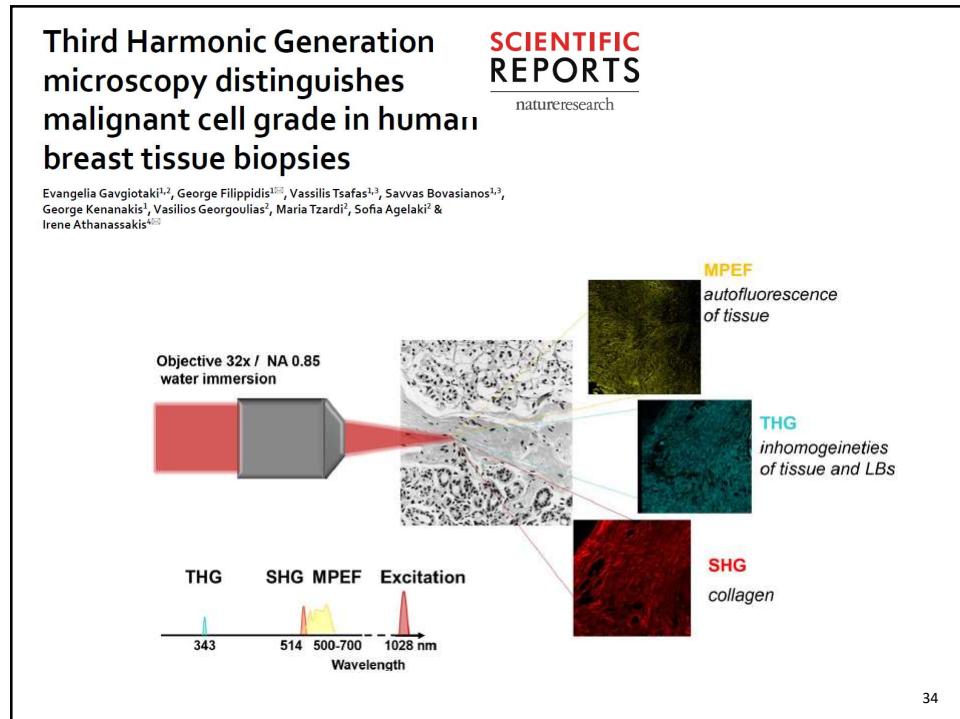
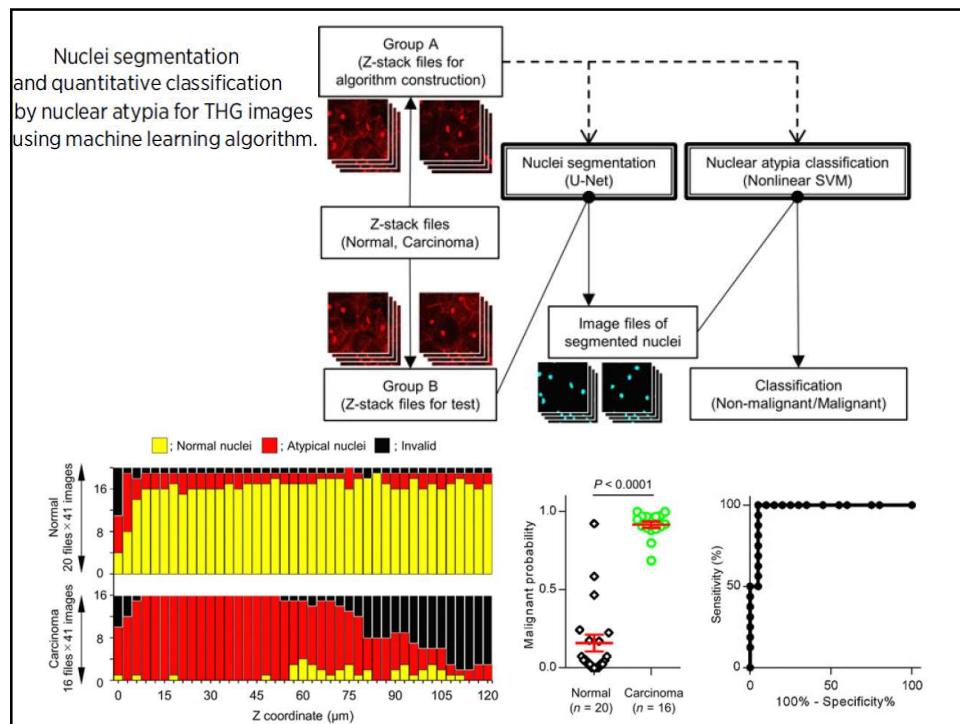
27

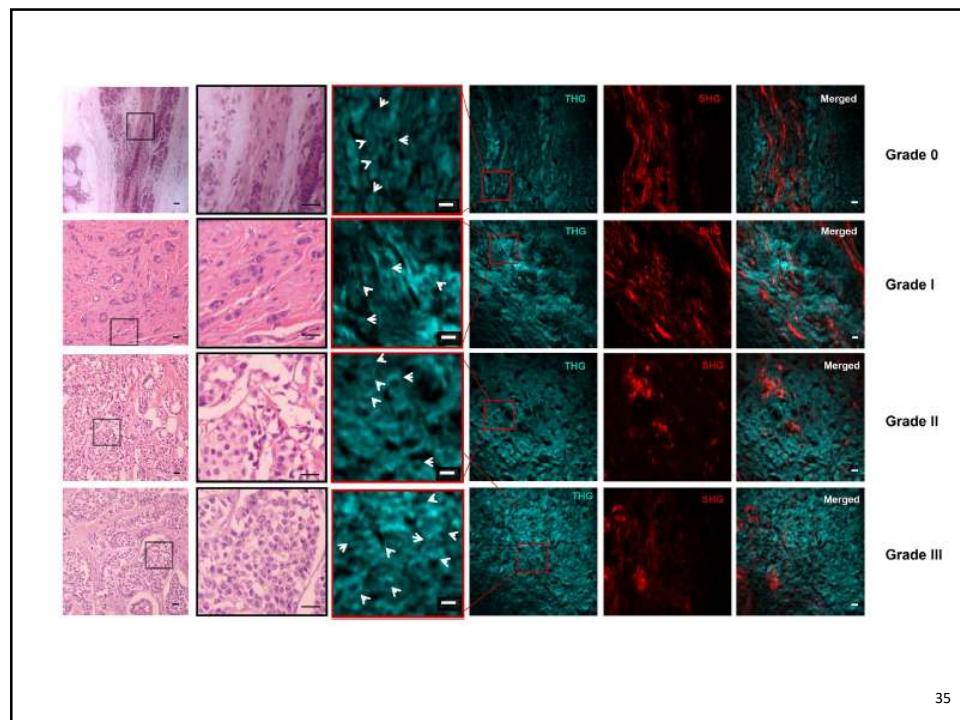
Table 2. Summary of TPEF and SHG imaging studies and techniques to probe collagen remodeling of the ECM in ovarian cancer.

TECHNIQUE	RESULTS	CONCLUSIONS	AUTHORS
GLCM on SHG images, spatial frequencies + TPEF redox ratios	GLCM Corr ₅₀ Normal and cancer statistically different	Variable redox ratios of high-risk women combined with collagen morphology may lead to improved detection	Kirkpatrick et al. ¹¹
Spatial frequency: Cancer tissues had increase in low ($\leq 10 \mu\text{m}^{-1}$) and decrease in high (72–92 μm^{-1}) spatial frequencies			
Redox ratio: Low risk > high risk > cancer			
Support vector machine (SVM) using GLCM, FFT	Classified cancer vs normal: Sensitivity = 81.5% Specificity = 81.1%	SVM of GLCM and FFT is moderately successful in classifying collagen alterations of cancerous tissues.	Watson et al. ³⁴
TPEF, SHG, and THG combined with FFT, TACS, and cellular signatures	FFT: Normal: 0.65 ± 0.12 Benign: 0.74 ± 0.11 Borderline: 0.80 ± 0.10 Serous: 0.79 ± 0.11 TACS: Normal and benign tumors demonstrate TACS-2 Serous demonstrate TACS-3	Multimodal imaging approaches are useful in classifying normal, benign, borderline, and serous ovarian tissues	Adur et al. ³¹
Texton classification	Classified normal and high-grade serous with 97% accuracy	Highly specific and versatile approach to classify ovarian tissues	Wen et al. ³⁵
SHG creation and anisotropy (β)	Type F_{SHG} β Normal 93% 0.76 Cancer 77% 0.88	Cancer is denser and more organized and has better packed fibrils than normal tissues	Nadiarnykh et al. ²⁹
Intravital TPEF and SHG imaging using STICK objective	Intrinsic tumor fluorescence is red-shifted relative to normal; Collagen is thicker in neoplasia lesions than normal tissues	Intravital TPEF and SHG imaging provides a means to detect small neoplastic regions using both collagen and cellular features	Williams et al. ¹³

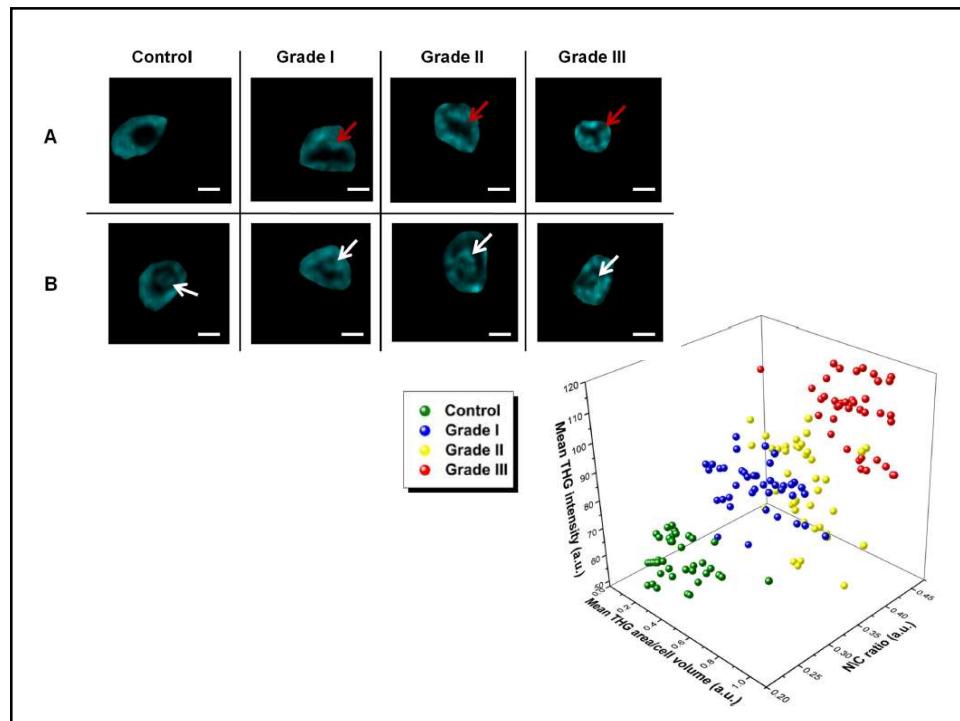


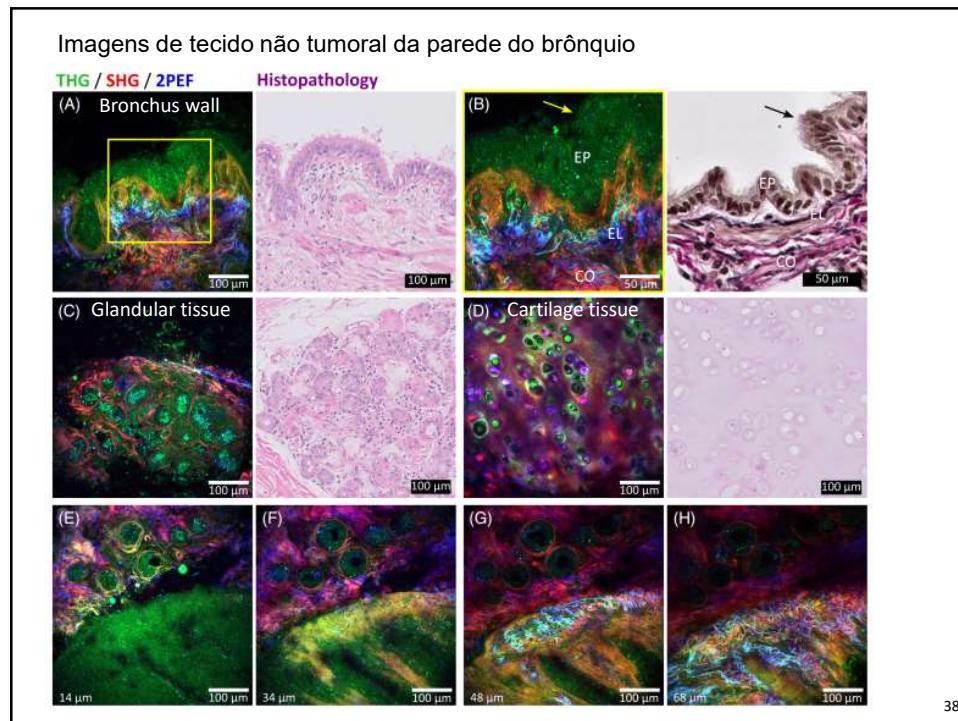
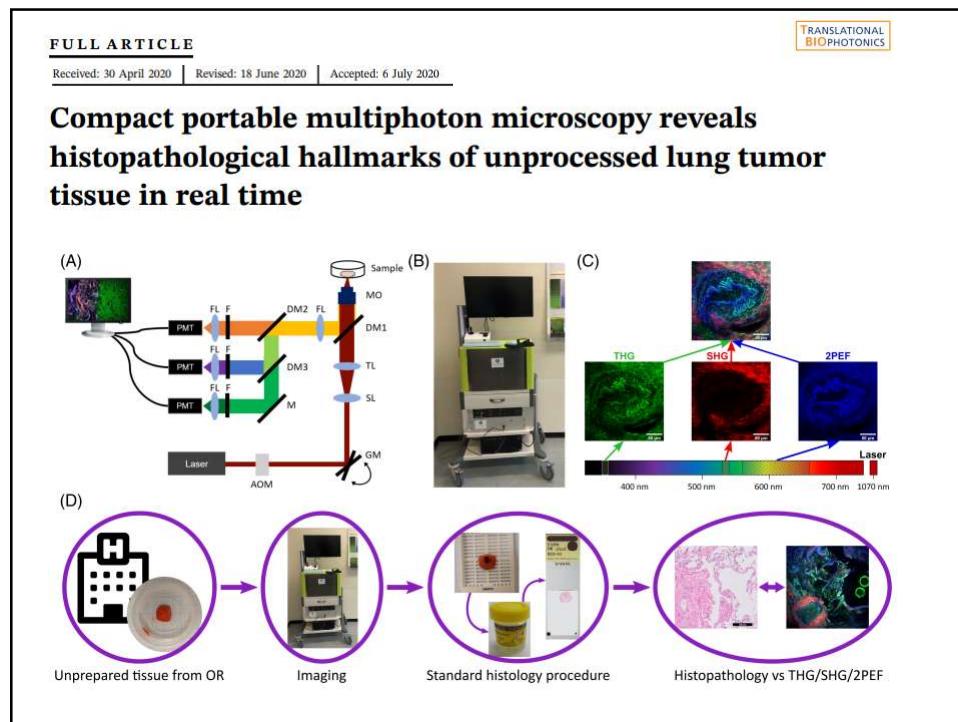


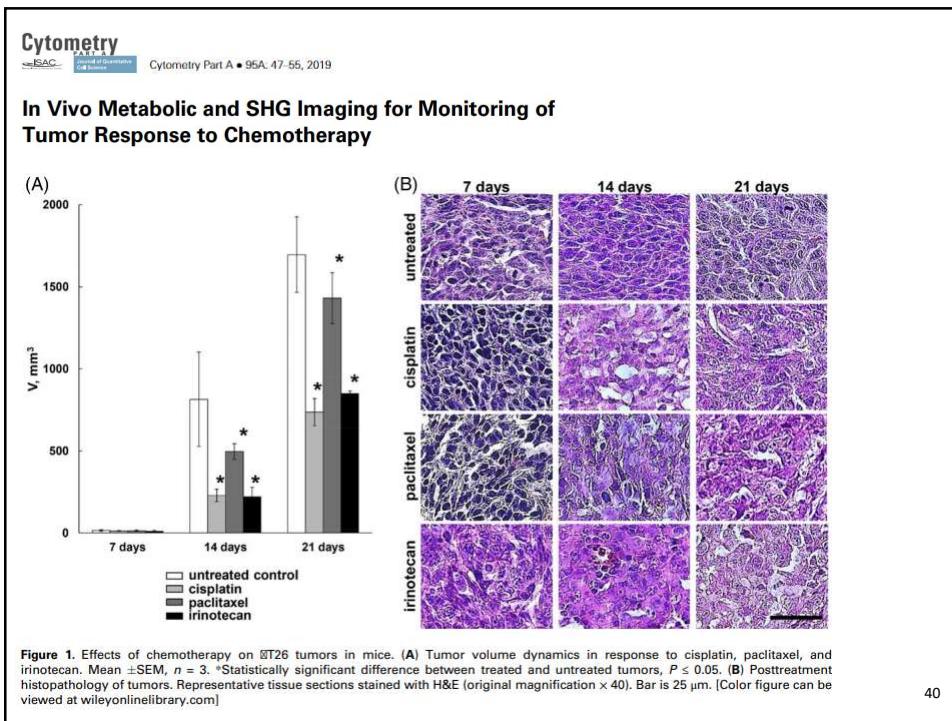
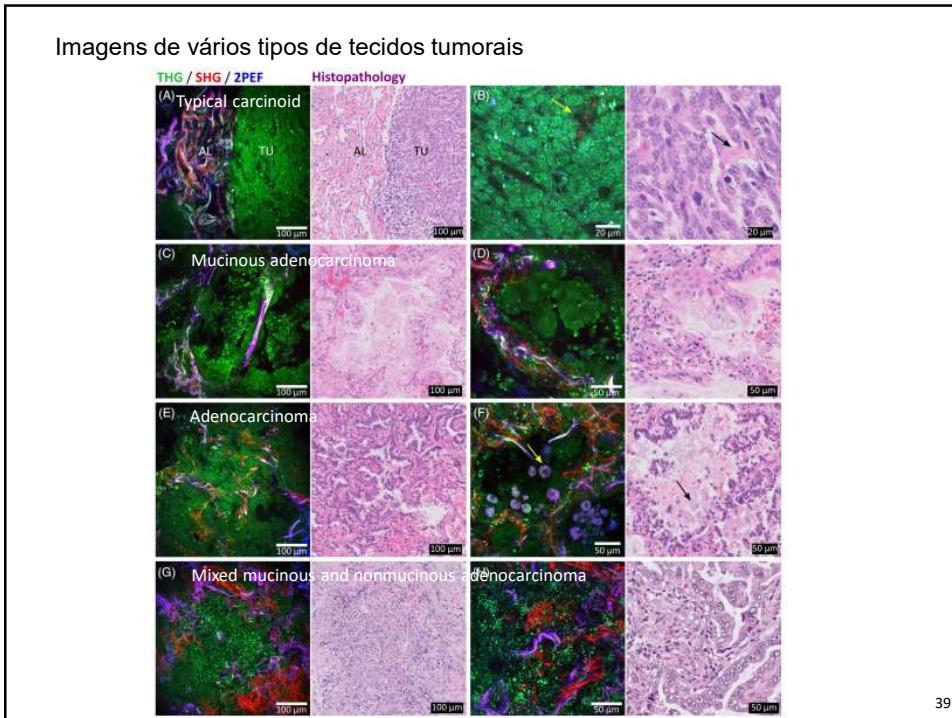


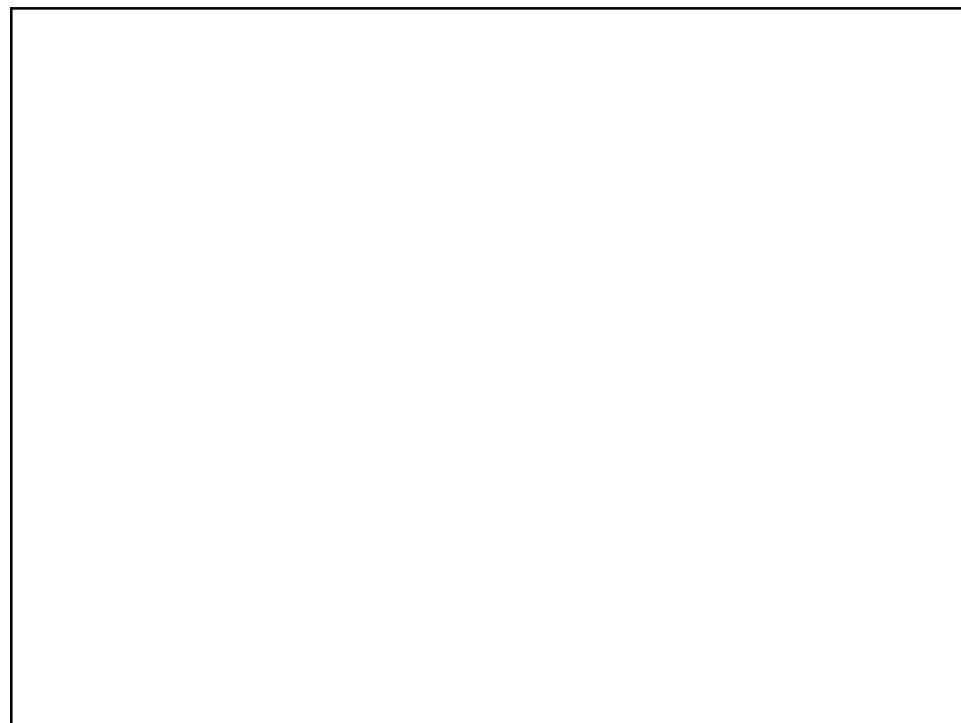
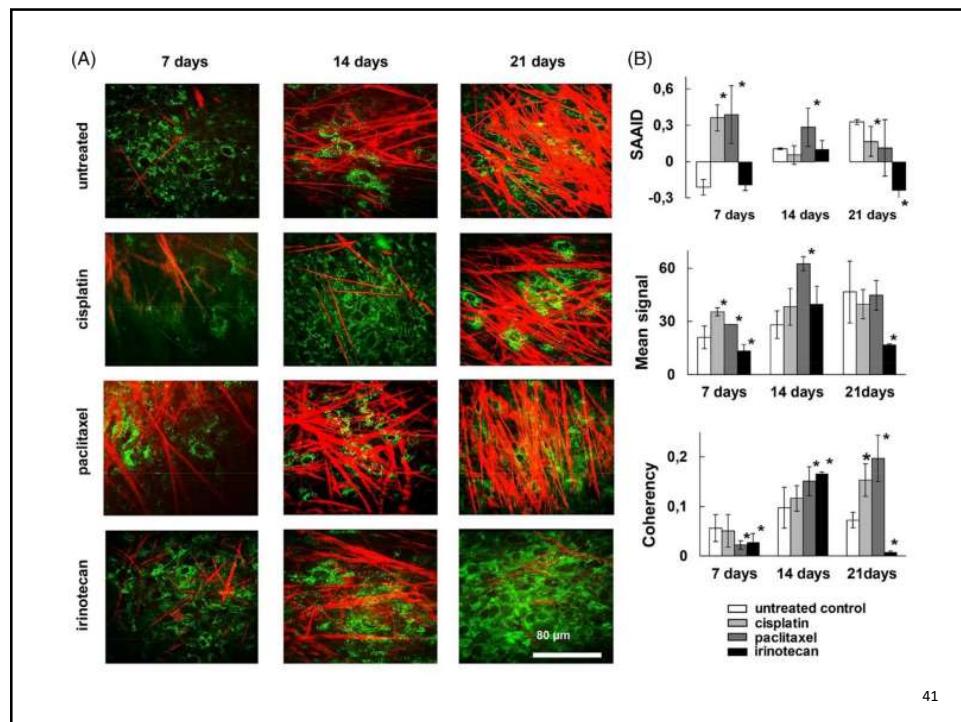


35











Obrigado por sua atenção...

javier.adur@uner.edu.ar